Catalysis Today xxx (2014) xxx–xxx

Contents lists available at ScienceDirect

Catalysis Today

journal homepage: www.elsevier.com/locate/cattod

Catalytic hydrodeoxygenation of anisole as lignin model compound over supported nickel catalysts

Shaohua Jin[a], Zihui Xiao[a], Chuang Li[a], Xiao Chen[a], Lei Wang[a], Jiacheng Xing[a], Wenzhen Li[b], Changhai Liang[a,*,1]

[a] Laboratory of Advanced Materials and Catalytic Engineering, School of Chemical Engineering, Dalian University of Technology, Dalian 116023, China
[b] Department of Chemical Engineering, Michigan Technological University, Houghton, USA

ARTICLE INFO

Article history:
Received 6 November 2013
Received in revised form 1 January 2014
Accepted 8 February 2014
Available online xxx

Keywords:
Hydrodeoxygenation
Anisole
Methoxy group
Lignin
Supported-nickel catalysts

ABSTRACT

Catalytic hydrodeoxygenation (HDO) of anisole, a methoxy-rich lignin model compound, has been investigated over a series of Ni-containing (10 wt% loading) catalysts with activated carbon, SBA-15, SiO_2, and γ-Al_2O_3 supports, in order to understand their ability for removal of —OCH_3 from anisole. This catalytic reaction had been carried out in an autoclave at 180–220 °C and 0.5–3.0 MPa H_2 pressure. Nickel-catalyzed aromatic ring-hydrogenation compared with the subsequent demethylation and deoxygenation is the fastest step in HDO of anisole under the present reaction conditions. Among these catalysts, the aromatic ring-saturated cyclohexyl methyl ether is mainly obtained over Ni/AC, while the Ni/SiO_2 displayed the highest activity in HDO of anisole (selectivity to deoxygenated products >95%). Differences in HDO efficiency among the catalysts are attributed not only to variations in the dispersion of the active phase, but also to the acid sites which may contribute to the cleavage of C—O bonds. It has also been shown that the activity toward oxygen-removal strongly depended on reaction temperature and the conversion of anisole favors the production of oxygen-free aromatics by the direct demethoxylation pathway at the relatively low H_2 pressure.

1. Introduction

Faced with the exhaustion of fossil fuel, great attention has been paid to develop a new-generation sustainable alternative energy. The utilization of biomass to produce bio-fuels and its derivative chemicals is an effective and sustainable way to relieve the energy crisis [1]. Numerous studies have been investigated to convert cellulose and hemicellulose to liquid fuels, such as alcohols or furan compounds [2,3]. However, only approximately two-thirds of the lignocellulosic biomass was utilized, as lignin occupies remaining 20–30% of total mass in the plants [4]. Lignin, as the most abundant renewable resources composed of aromatic units in nature, and the largest contributor to soil organic matter, can be broken down to phenolic monomers by catalytic and thermochemical processes [5]. However, these phenolic compounds cannot be used as a liquid fuel directly owing to their high oxygen content, poor chemical stability, corrosivity to the equipment [1].

Catalytic hydrodeoxygenation is considered to be one of the most effective routes for lignin-derived bio-oils upgrading [6]. Among the characteristic groups of lignin, methoxy group which associated with phenylpropane, syringyl and guaiacyl units (as shown in Scheme 1), is one of the major functional groups and has different reactivities in chemical reactions [7]. Although lots of works have been studied on the catalytic conversion of lignin model compounds, the reports on the hydrodeoxygenation of methoxy-rich compounds were limited. Consequently, it is particularly important to find an effective catalyst for removal of aromatic carbon–oxygen (C—O) bonds. Conventional sulfide NiMo and CoMo/γ-Al_2O_3 catalysts have been studied for catalytic hydrotreatment of bio-oils and their model compounds [8–10]. Noble metal catalysts, such as Pt/C, Pt-Sn/CNFs, Pd, Ru, Rh/SiO_2-Al_2O_3 [11–13], also exhibited excellent activities for HDO of lignin-derived chemicals. However, sulfided catalysts are potentially problematic due to sulfur contamination to the final products, water-induced catalyst deactivation and coke accumulation [14]. In addition, the high cost of noble metal catalysts also limits their wide application. Nickel-based catalysts, including nickel phosphide [15–18], seem to be a promising noble-metal free catalytic system that can satisfy the HDO process requirements, such as low cost, non-sulfided nature and high activity [19].

* Corresponding author. Fax: +86 411 84986353.
E-mail address: changhai@dlut.edu.cn (C. Liang).
[1] http://finechem.dlut.edu.cn/liangchanghai.

http://dx.doi.org/10.1016/j.cattod.2014.02.014
0920-5861/

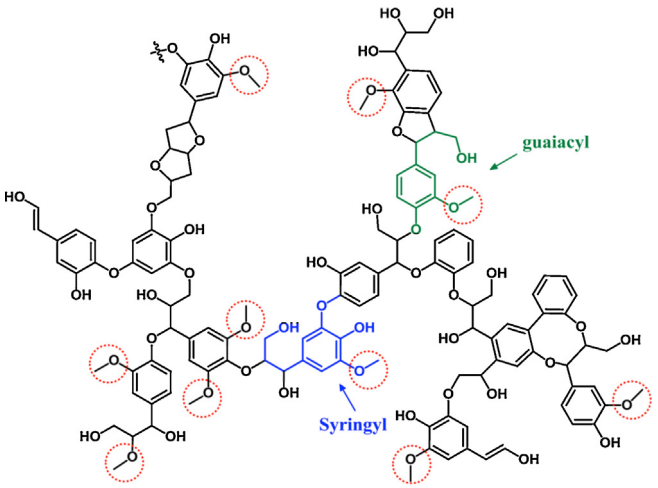

Scheme 1. Schematic representation of a typical lignin fragment.

Various catalyst supports appear to play a significant role in deoxygenation of the lignin monomers. Ohta et al. found carbon-supported Pt showed high activity and durability in the HDO of phenols [11]. γ-Al_2O_3 effectively promoted dehydration reaction of the alcohol produced from hydrogenation of the aromatic ring [20]. Mesoporous silica materials, in particular SBA-15, have generated interests as catalyst supports in the HDO of a biomass-derived compounds due to their high structure regularity, low-cost and non-toxicity [21]. SiO_2 supported Fe also showed good activity and selectivity toward conversion of guaiacol into aromatic hydrocarbons [22]. However, a limited number of studies have been performed on the effects of catalyst supports for the hydrotreating of methoxy-rich lignin model compounds.

For those reasons, herein we report a screening study on the catalytic HDO of methoxy-rich lignin model compound anisole over Ni nanoparticles dispersed on different supports (active carbon, γ-Al_2O_3, SiO_2 and SBA-15) under mild conditions (210 °C, 3.0 MPa), in order to understand the effect of supports on the activity toward the removal of oxygen from anisole.

2. Experimental

2.1. Catalyst preparation

SBA-15 mesoporous silica was synthesized following a reported procedure [23]. The other three supports active carbon (AC), γ-Al_2O_3, SiO_2 were purchased commercially. Before use, the AC supports were washed to remove the impurities in a 0.5 mol/L aqueous nitric acid solution at room temperature for 24 h. The support powders were all sieved to obtain particles smaller than 100 meshes before use and dried in air at 140 °C overnight. The 10 wt% Ni catalysts supported on AC, SiO_2, γ-Al_2O_3 and SBA-15 were prepared by an incipient impregnation method using the aqueous solution of the metal salt $Ni(NO_3)_2{\cdot}6H_2O$. The precursor solutions were added dropwise to the supports. After the impregnation, the catalysts were dried at 110 °C in air for 12 h and then calcined at 400 °C in Ar for 3 h.

2.2. Catalyst characterization

The content of Ni was measured by inductively coupled plasma-optical emission spectroscopy (ICP-OES). After dissolved with nitromurlatic acid solution, the samples were filtered and analyzed by ICP-OES. The phase structure of the samples was obtained by powder X-ray diffraction (XRD) analysis in a D/MAX-2400 diffractometer using a Cu Kα radiation (λ = 1.5418 Å), operated at 40 kV and 100 mA. Temperature-programmed reduction of hydrogen (H_2-TPR) was performed in a stream of 10% H_2 in Ar with a flow rate of 50 cm^3/min. The samples were heated up to a final temperature of 900 °C at 10 °C/min and H_2 consumption was monitored by a thermal conductivity detector. In the case of NH_3-TPD experiments, the reduced catalysts were outgassed in He at 350 °C for 0.5 h, and finally saturated at 100 °C in a 10% NH_3/He stream (50 ml/min) for 1 h. After removing most weakly physisorbed NH_3 by flowing He (50 ml/min) for 30 min, the chemisorbed ammonia was determined by using TCD by heating at 10 °C/min up to 700 °C under the same flow of He. BET surface areas, pore volumes and pore size distributions of the catalysts (approximately 0.1 g sample) were determined by nitrogen physisorption at liquid N_2 temperature with a autosorb iQ automated gas sorption analyzer. The amounts of metal active sites were estimated from irreversible CO adsorption measurements performed at room temperature. Typically, the catalyst samples were reduced in a 10% H_2/He at 400 °C, followed by exposure to flowing He for 2 h. CO adsorption was conducted when the sample was cooled to room temperature. Then, the samples were purged by the flowing He for 1 h, and CO adsorption was repeated. The particle size and dispersion of the samples were analyzed by transmission electron microscopy (TEM). Powder samples were ultrasonicated in ethanol and dispersed on holey carbon films on copper grids.

2.3. Anisole HDO and product analysis

Anisole HDO was carried out in a 50 mL stainless steel autoclave equipped with a magnetic stirrer and an electric temperature controller. Prior to reaction, the obtained Ni-based catalysts were reduced by H_2 at 400 °C for 2 h and then passivated in Ar overnight. 8 wt% anisole (1.2 g, 0.0108 mol) dissolved in 20 mL *n*-decane with 2 wt% *n*-dodecane as an internal standard for quantitative GC analysis and 0.1 g reduced catalysts were rapidly introduced into the autoclave to prevent from contacting with air for long. Afterwards, the autoclave was sealed and purged repeatedly with H_2 to eliminate air, pressurized to the desired hydrogen pressure and then heated to the desired temperature at 700 rpm stirring speed. The zero time point was defined when the autoclave was heated. It takes about 30 min to reach reaction temperature. The autoclave was cooled to room temperature and brought to ambient pressure after the reaction was finished. The products were analyzed by gas chromatograph (GC-7890F, FID, FFAP column 30 m × 0.32 mm × 0.5 μm) and identified by a GC–MS (Agilent 6890, HP-5 MS capillary column, 30 m × 0.25 mm × 0.25 μm).

3. Results and discussion

3.1. Catalyst properties

For all catalysts, the chemical analysis reveals that the actual metal loading is almost close to the theoretical value of 10%, as shown in Table 1. N_2 sorption analyses were performed to determine the differences in support morphology of all catalysts. The N_2 adsorption–desorption isotherms and pore size distributions (PSD) of all catalysts after calcination are shown in Fig. 1. AC and SiO_2 supported Ni catalysts both showed a typical Type I isotherm according to the IUPAC classification, suggesting a large number of micropores existed, which also can be obtained from the PSD support. In addition, PSD curves of Ni/AC and SiO_2 showed the presence of small mesopores (smaller than 4 nm). Owing to the presence of abundant micropores, Ni/AC and Ni/SiO_2 had a high surface area of 1293 and 549 m^2/g. Compare with Ni/SiO_2, Ni/AC owned much more micropores and larger pore volume of 0.6 cm^3/g. As-synthesized SBA-15

Please cite this article in press as: S. Jin, et al., Catalytic hydrodeoxygenation of anisole as lignin model compound over supported nickel catalysts, Catal. Today (2014), http://dx.doi.org/10.1016/j.cattod.2014.02.014

Table 1
Chemical and structure properties of the supported Ni catalysts.

Catalyst	ICP-OES[a] (wt%)	S_{BET}[b] (m^2/g)	d (nm)[b]	V_{meso}[b] (cm^3/g)	V_{total}[b] (cm^3/g)
Ni/AC	10.2	1293	1.9	0.22	0.60
Ni/γ-Al_2O_3	9.3	229	7.0	0.34	0.40
Ni/SBA-15	10.3	662	6.0	0.85	1.00
Ni/SiO_2	9.0	549	2.2	0.16	0.31

[a] As determined by the ICP-OES technique.
[b] BET surface area (S_{BET}), average pore diameter (d) and total pore volume (V_{total}) as determined by N_2 adsorption–desorption isotherms at −196 °C.

supported Ni catalyst displayed a Type IV isotherm and standard H1 type hysteresis loop by IUPAC classification, showing that the existence of a highly ordered mesopores. The isotherms for the Ni/SBA-15 materials showed a sharp inflection in the relative pressure (P/P_0) range from 0.7 to 0.8, reflecting the presence of uniform PSD [24]. Due to well-defined mesoporosity of SBA-15, a high surface area of 662 m^2/g and narrow pore size distribution with an average diameter of 8.2 nm (see Fig. 1c). Porous Ni/γ-Al_2O_3 catalyst had a BET specific surface area of 230 m^2/g and total pore volume of 0.4 cm^3/g. It contained both micropores and mesopores, with a narrow micropore size distribution centered at 1 nm and a wide mesopore size distribution from 3 to 8 nm, as shown in Fig. 1b.

The wide-angel XRD technique was performed to study the formation of crystalline species for different supports loaded Ni catalysts after reduction at 400 °C for 2 h. Owing to the formation of metallic nickel, the XRD patterns (Fig. 2) of reduced Ni/AC, Ni/SBA-15 and Ni/SiO_2 catalysts show peaks at 2θ of 45.5°, 51.9°, 76.3°, respectively corresponding to lattice plane (1 1 1), (2 0 0) and (2 2 0) of metallic nickel (JCPDS 04-0850), along with amorphous and broad active carbon peaks centered at 2θ of 23° and 43° and SiO_2 diffraction peaks centered at 2θ of 23°. While Ni peaks of SBA-15 catalysts are sharper than that of other catalysts, indicating the

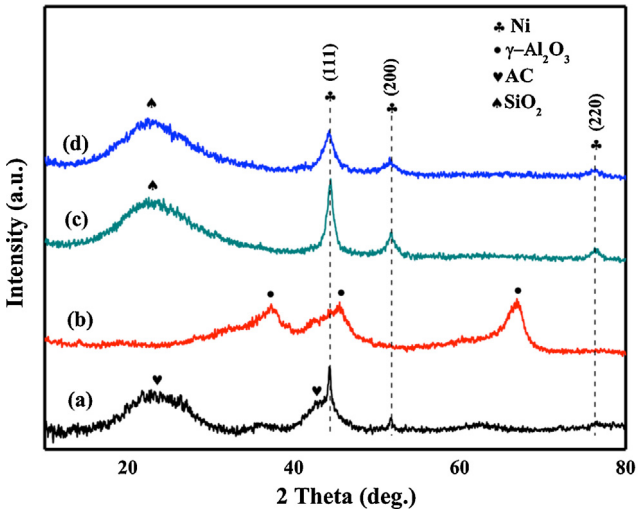

Fig. 2. X-ray diffraction patterns of (a) Ni/AC, (b) Ni/γ-Al_2O_3, (c) Ni/SBA-15 and (d) Ni/SiO_2 after reduction.

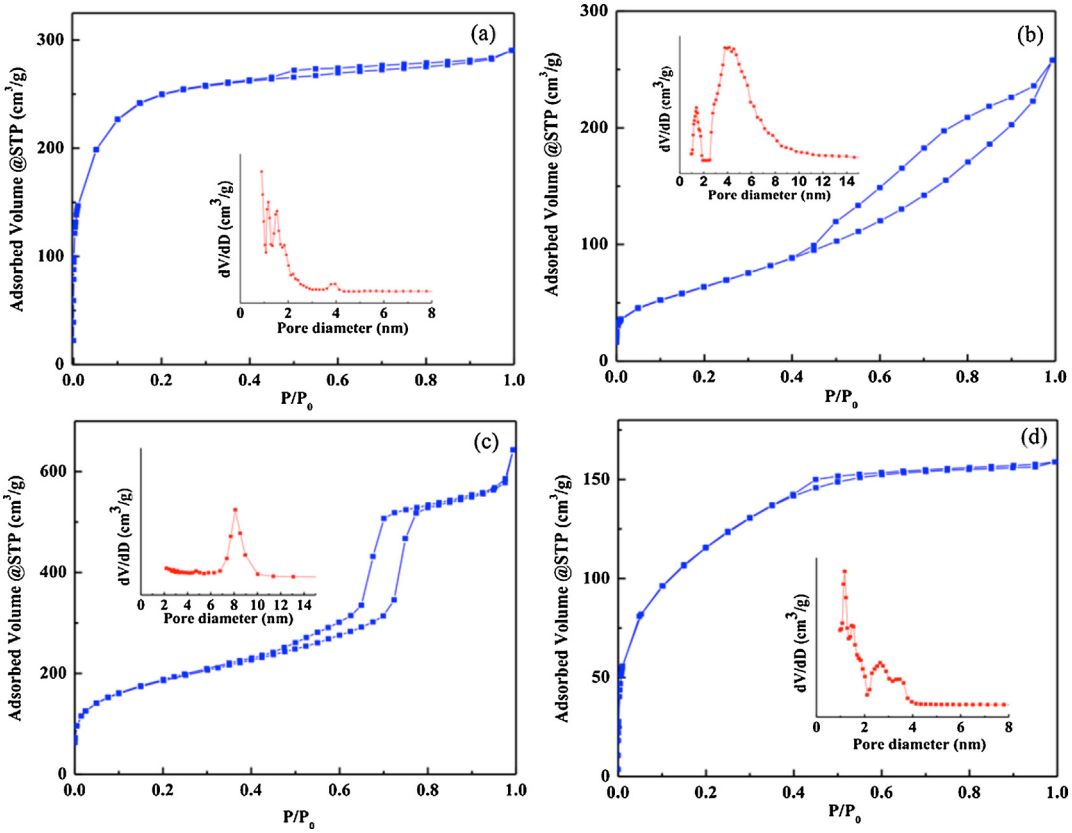

Fig. 1. N_2 adsorption/desorption isotherms with DFT pore size distributions ((a) 10% Ni/AC; (b) 10% Ni/γ-Al_2O_3; (d) 10% Ni/SiO_2) and BJH pore size distributions ((c) 10% Ni/SBA-15) derived from the adsorption branches of the isotherms.

Please cite this article in press as: S. Jin, et al., Catalytic hydrodeoxygenation of anisole as lignin model compound over supported nickel catalysts, Catal. Today (2014), http://dx.doi.org/10.1016/j.cattod.2014.02.014

existence of larger clusters. Fig. 2b mainly shows peaks of γ-Al_2O_3, with unapparent peaks of metallic Ni or NiO, suggesting the existence of very small particles [25], which is also consistent with its TEM result. On the other hand, because of the strong interaction between nickel particles and γ-Al_2O_3 and the formation of an amorphous surface nickel aluminate [25–27], the complete exposition of activity phase of Ni/γ-Al_2O_3 may need higher reduction temperature.

H_2-TPR profiles of Ni catalysts on different supports are shown in Fig. 3. The reduction peak at 365 °C for Ni/AC and Ni/SBA-15, at 390 °C for Ni/SiO_2 and at 430 °C Ni/γ-Al_2O_3, usually assigned to the reduction of NiO clusters interacting weakly with the supports [28]. In the case of Ni/AC, the second peak at 500 °C is attributed to the reduction of highly dispersed NiO interacted with AC, which is partially overlapped with the peaks of carbon methanation and CO_2 or CO from O-containing functional groups on the surface of AC supports. For the Ni/γ-Al_2O_3 catalyst, it has a peak at 570 °C, which indicates the presence of NiO contacted strongly with γ-Al_2O_3. The reduction of Ni/γ-Al_2O_3 catalyst displays a similar behavior compared to the results in the reference, but is highly dependent on the TPR conditions employed [25,29]. The reduction profile of Ni/SiO_2 is very similar to Ni/SBA-15, showing a broad peak centered at 624 °C, which is because of the reduction of highly dispersed NiO contacted strongly with the silica materials or nickel silicates formed during

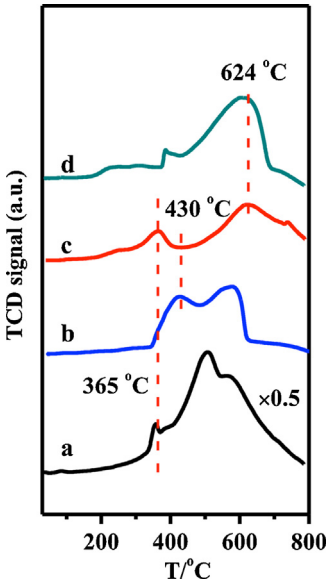

Fig. 3. H_2-TPR profiles of (a) Ni/AC, (b) Ni/γ-Al_2O_3, (c) Ni/SBA-15 and (d) Ni/SiO_2 after calcined in Ar at 400 °C.

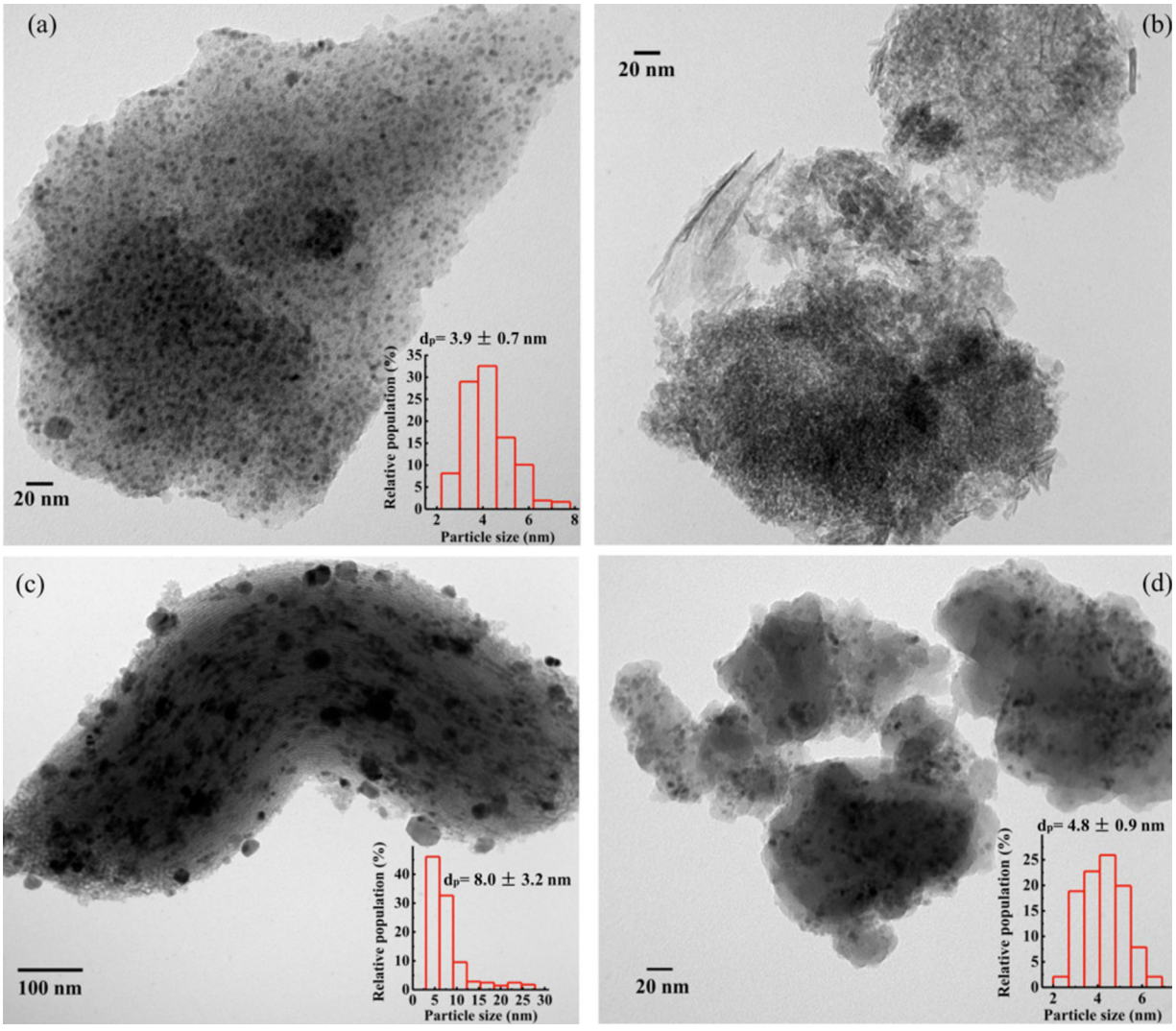

Fig. 4. TEM images of the reduced (a) Ni/AC, (b) Ni/γ-Al_2O_3, (c) Ni/SBA-15 and (d) Ni/SiO_2.

Please cite this article in press as: S. Jin, et al., Catalytic hydrodeoxygenation of anisole as lignin model compound over supported nickel catalysts, Catal. Today (2014), http://dx.doi.org/10.1016/j.cattod.2014.02.014

Table 2
CO chemisorption and metallic particle sizes of the supported Ni catalysts.

Catalyst	CO uptake[a] (μmol/g cat.)	D%[a]	d_{CO}[a]	d_{XRD}[b]	d_{TEM}[c]
Ni/AC	292	18.3	5.5	–	3.9
Ni/γ-Al_2O_3	163	–	–	–	–
Ni/SBA-15	190	12.5	8.1	8.4	8.0
Ni/SiO_2	205	14.4	6.0	5.7	4.8

[a] CO uptake, dispersion (*D*%) and average particle size (d_{CO}) as measured by CO chemisorption at room temperature.
[b] Average particle size (d_{XRD}) calculated by using the Scherrer equation by XRD.
[c] Average particle size (d_{TEM}) obtained from TEM.

calcination. Therefore, the H_2-TPR results indicate that the strong interactions between nickel and supports would happen when the metal salt $Ni(NO_3)_2{\cdot}6H_2O$ impregnated in supports and then calcined at 400 °C in Ar.

TEM technique was conducted to study the distribution of nickel particles on these four supports. Fig. 4 shows their TEM images together with the histograms of particle size of the reduced Ni catalysts. The results indicate that Ni particles are well-distributed all over the AC, SBA-15, SiO_2 and γ-Al_2O_3. For AC catalyst, owing to its largest surface area of 1293 cm^3/g, the size is smaller than the rest of the catalysts, with a relatively narrow size distribution. For γ-Al_2O_3 catalyst, it is not easy to make a statistics of particle size distribution, due to a less clear distinction between Ni and support. However, some irregular Ni particles with mainly globular morphology can be distinguished due to the darkest contrast. SBA-15 catalysts show hexagonal cylinder-like morphologies. A portion of nickel species entered into its cylinder-like pores, exhibiting a strip-type distribution. While a small amount of Ni particles inevitably aggregated outside the SBA-15 when calcined in Ar at 400 °C. The SiO_2 catalyst exhibits the similar situation to the AC catalyst, while its mean particle diameter is slightly larger than that of the former catalyst, which is likely due to the smaller surface area of 549 cm^3/g. The average size of metal particles, as calculated by statistical analysis of about 200 particles, is also showed in Fig. 4. The metal particle size follows the trend Ni/SBA-15 (8.0 ± 3.2 nm) > Ni/SiO_2 (4.8 ± 0.9 nm) > Ni/AC (3.9 ± 0.7 nm).

The amounts of metal active sites were estimated from irreversible CO chemisorption measurement and the results are listed in Table 2, which also summarizes the Ni particle sizes calculated from XRD, CO chemisorption and TEM. We can see that Ni/AC catalyst has the best metal dispersion and smallest Ni particle size owing to its large surface area of 1293 m^2/g. In addition, the Ni particle size has a similar tendency ($d_{SBA\text{-}15} > d_{SiO_2} > d_{AC}$) calculated from these three methods. However, for γ-Al_2O_3, due to the interference of support peaks and the formation of difficult-reduced nickel aluminate, it is not easy to calculate the Ni particle size according to these three methods.

The acidity of all catalysts was determined by temperature-programmed desorption of ammonia (NH_3-TPD) and desorption profiles are displayed in Fig. 5. For Ni/AC catalyst, it does not exhibit weak NH_3 desorption feature below 500 °C and only shows a sharp peak at around 520 °C, which can be attributed to the TCD signals of CO_2 or CO formed by carbon oxidization with O-containing functional groups located on the surface of AC supports, because this peak also exists when the measure was performed in pure He. In other cases, Ni/SBA-15 and Ni/SiO_2 exhibit the similar TPD profiles and present three main peaks which are centered at 200 °C, 400 °C and 620 °C separately. Similarly, Ni/γ-Al_2O_3 presents two prominent and broad peaks respectively centered at 260 °C and 570 °C, which could be associated with weak acidic sites and stronger acidic sites [30].

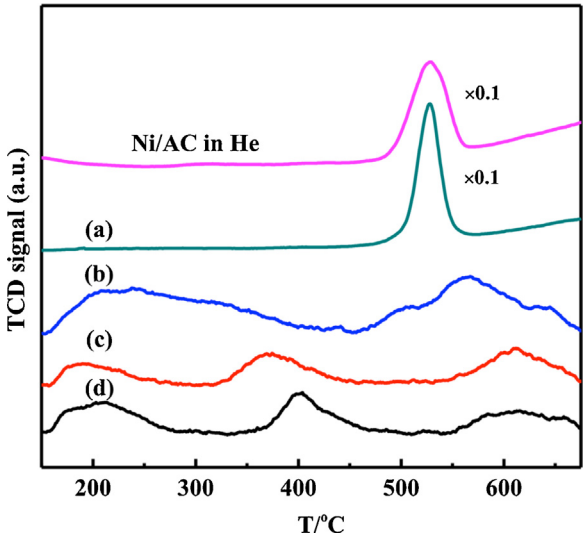

Fig. 5. NH_3-TPD profiles of the reduced Ni/AC(a), Ni/γ-Al_2O_3(b), Ni/SBA-15(c) and Ni/SiO_2(d).

3.2. Catalytic activity

In the present study, we evaluated and compared the catalytic performance of Ni/AC, Ni/γ-Al_2O_3, Ni/SBA-15, Ni/SiO_2 in HDO of methoxy-rich compound anisole. Fig. 6 shows the variation of the conversion of anisole and the yield of products with time. All these experiments were performed at least in duplicate and the results were well reproducible. The main products detected by GC–MS and GC are cyclohexyl methyl ether (CME), cyclohexanol (CHL), cyclohexane (CHE), cyclohexyl cyclohexyl ether (CCE). In addition, small amounts of the directly demethoxylated products benzene (BEN) and methanol can also be detected. Overall, the main anisole conversion pathways under the current conditions mainly consist of three steps. The first step is the hydrogenation saturation of aromatic ring of anisole, followed by the second step of demethylation by the hydrogenolysis of the O—CH_3 bond of the methoxy group, resulting in the formation of cyclohexanol. The last step is the deoxygenation of cyclohexanol to produce cyclohexane by the intramolecular dehydration reaction of hydroxyl group. Otherwise, small amounts of CCE were also obtained by the intermolecular dehydration reaction of two cyclohexanol molecules.

From the results shown in Fig. 6, we can see that the feedstock anisole were almost completely converted within 90 min for all four Ni catalysts. Except the Ni/SiO_2, the main products obtained from anisole are aromatic ring-hydrogenated CME, however subsequently the degree of demethylation and deoxygenation with time going by is quite different depending on the supports. These results suggest that the fastest step in HDO of anisole is the nickel-catalyzed aromatic ring-hydrogenation rather than the subsequent demethylation and deoxygenation [1]. Ni/AC in the current conditions presents a relatively low HDO yield, due to the moderate capacity for the hydrogenolysis of the C—O bonds. After 225 min, the selectivity of O-free CHN is only 15%, while a selectivity of 71% CME was accumulated, which shows that Ni/AC has a poor hydrodeoxygenation (HDO) efficiency even though its ability for aromatic-ring hydrogenation is excellent. Although Ni/γ-Al_2O_3 owns more relatively strong acid sites for the cleavage of the C—O bonds, due to the existence of the hardly-reduced Ni species, the subdued synergetic catalytic effect between acid sites for hydrogenolysis and metal sites for hydrogenation prevents the dehydration of CHL to CHN. As a result, compared with other three catalysts, relatively more demethylated product CHL with a selectivity of 14.1% was obtained. Compared with Ni/AC and Ni/γ-Al_2O_3, Ni catalysts supported on

Please cite this article in press as: S. Jin, et al., Catalytic hydrodeoxygenation of anisole as lignin model compound over supported nickel catalysts, Catal. Today (2014), http://dx.doi.org/10.1016/j.cattod.2014.02.014

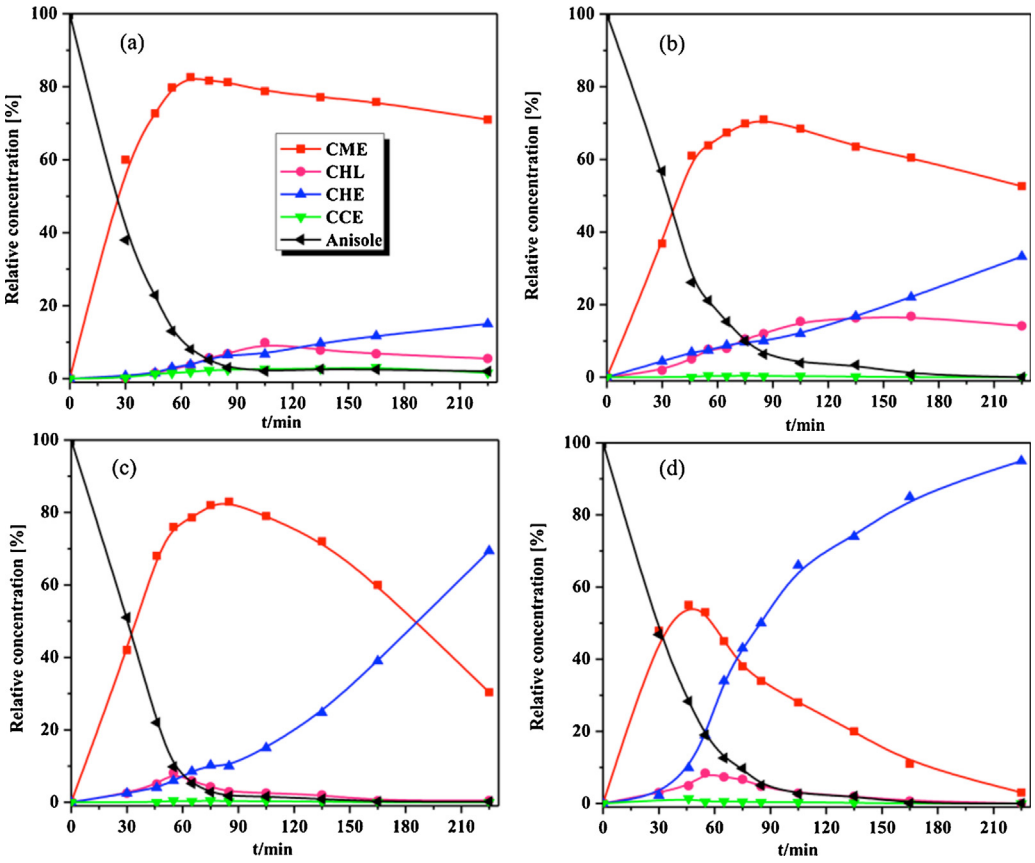

Fig. 6. Variation of the conversion of anisole and the yield of products with time for (a) Ni/AC, (b) Ni/γ-Al_2O_3, (c) Ni/SBA-15 and (d) Ni/SiO_2.

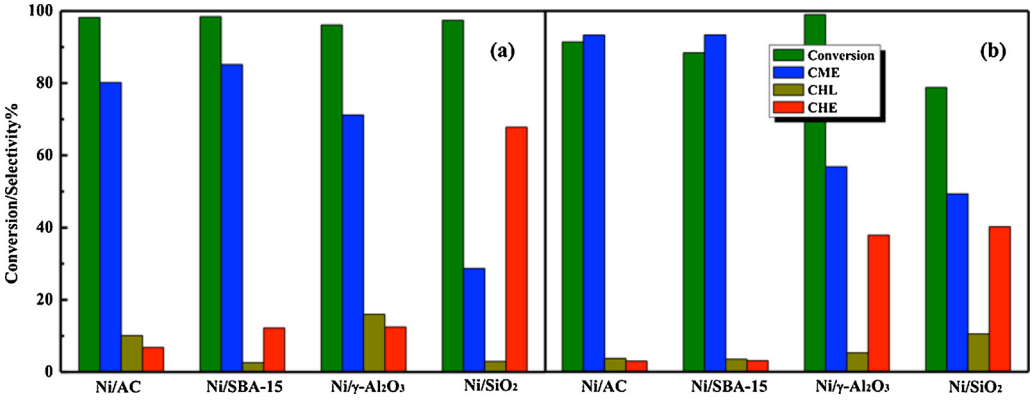

Fig. 7. Reduction temperature dependence of conversion and selectivity to main products in HDO of anisole.

silica materials exhibited a better deoxygenation activity with a HDO% of 70% for Ni/SBA-15 and 95% for Ni/SiO_2, which appears to be related to the favorable synergetic catalytic effect between acid sites and metal sites [13,20]. On the other hand, the weak acidic OH sites located on the surface of silica materials favor the adsorption with O atoms in hydroxyl or methoxy groups, which is also responsible for excellent ability for the cleavage of C—O [22].

To further study the reducibility of all the catalysts, reduction temperature dependence of conversion of anisole was investigated, as shown in Fig. 7. According to the activity results, the conversion of anisole and HDO yields both clearly decrease for Ni/AC, SBA-15 and SiO_2, indicating that the increase of reduction temperature weakens the hydrogenation capacity of these catalysts, which is owing to the existence of larger Ni particles by the inevitable aggregation at the high temperature. Nevertheless, Ni/γ-Al_2O_3 exhibits even higher anisole conversion and yield of deoxygenated products CHN when reduced at 500 °C. It is because the release of more Ni particles obtained from hardly-reduced Ni species of this catalyst results in stronger synergetic catalytic effect between acid sites and metal sites.

Since it demonstrates the best deoxygenation activity in the HDO process of anisole [31], Ni/SiO_2 catalyst was used to investigate the effect of temperature on the product distribution and effectiveness of the overall process. The corresponding results are shown in Fig. 8. The feedstock anisole was almost completely transformed at the temperature range of 180–220 °C under the current conditions. As the aromatic ring hydrogenation process is a fast step, the main products in HDO of anisole catalyzed by Ni/SiO_2 are non-aromatic hydrocarbon, i.e. oxygenous alkane and oxygen-free alkane. From the results in Fig. 8, we can see that the

Please cite this article in press as: S. Jin, et al., Catalytic hydrodeoxygenation of anisole as lignin model compound over supported nickel catalysts, Catal. Today (2014), http://dx.doi.org/10.1016/j.cattod.2014.02.014

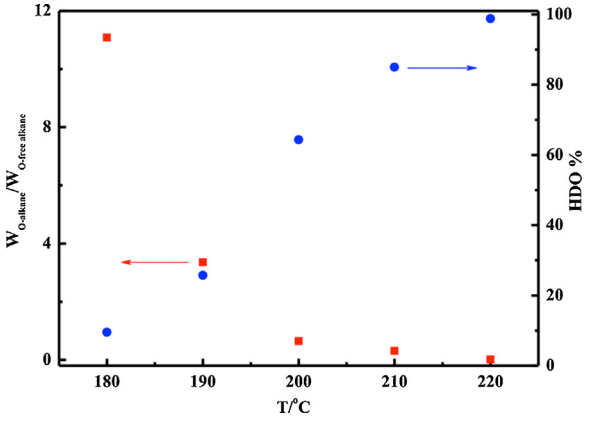

Fig. 8. Effect of temperature on the ratio of oxygenous alkane to oxygen-free alkane ($W_{O\text{-alkane}}/W_{O\text{-free alkane}}$) and the deoxygenation degree in HDO of anisole.

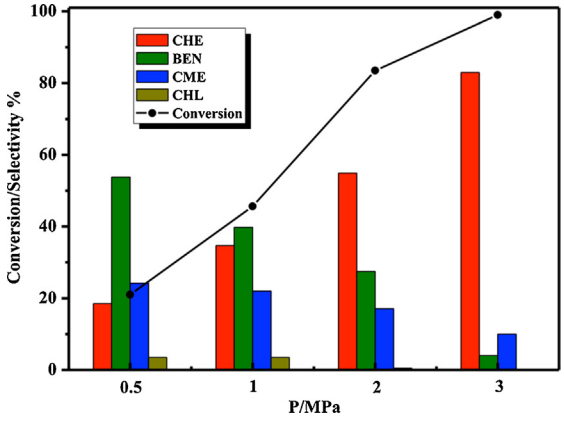

Fig. 9. Pressure dependence of conversion and selectivity toward main products in HDO of anisole.

deoxygenation activity of Ni/SiO_2 strongly depends on reaction temperature. At the low temperature of 180 °C, the products mainly consist of oxygenous alkane CME. With the increase of temperature, the ratio of oxygen-free alkane to oxygenous alkane and HDO% of anisole both increase. At the high temperature of 220 °C, the oxygen-free alkane CHE is the main product in the target process (HDO) and simultaneously the HDO% of anisole reaches up to 99%.

The pressure dependence of conversion and selectivity toward main products in HDO of anisole over Ni/SiO_2 is shown in Fig. 9. We can easily get a conclusion that the pressure plays a significant role on both anisole conversion and main products distribution. With increasing hydrogen pressure from 0.5 to 3.0 MPa, the conversion of anisole increases from 22% to 99%. At the high hydrogen pressure, the hydrogenation saturation of aromatic ring and subsequent deoxygenation process can be easily achieved. Nevertheless, it becomes difficult to carry out the aromatic ring-hydrogenation process at the low hydrogen pressure. At present, the direct demethoxylation pathway stands out and the selectivity of BEN at 0.5 MPa reaches to 53%. According to the reported works [12,32], we can get the same conclusion that at the low pressure, even at the atmospheric pressure, it favors the production of oxygen-free aromatics by the direct demethoxylation process.

According to the previous results, the reaction network for anisole HDO over Ni catalysts in the current conditions is presented in Scheme 2. At the sufficient H_2 pressure, the hydrogenation saturation of aromatic ring of anisole is easy to conduct for all four Ni catalysts. However, the supports exhibit significant influence in subsequent demethylation and deoxygenation to produce O-free CHN. Moreover, the intermolecular dehydration reaction of

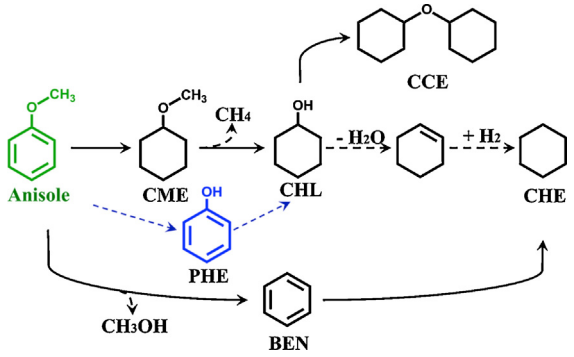

Scheme 2. Reaction network of anisole hydrodeoxygenation over supported Ni catalysts.

two cyclohexanol molecules can also happen over Ni/AC. At the deficient H_2 pressure, the removal of —OCH_3 from anisole to form benzene by direct demethoxylation can be achieved. Furthermore, the direct demethylation process of anisole to produce phenols (PHE) [15] can also occur, while unfortunately this intermediate product is not detected by GC–MS, which may be related to faster phenol hydrogenation rate than its formation rate on the Ni catalysts.

4. Conclusions

Supported nickel catalysts with a broad range of physicochemical properties obtained by an incipient impregnation technique have been evaluated in hydrodeoxygenation of methoxy-rich lignin model compound anisole in a batch set-up. The catalysts exhibit the high activity toward the hydrogenation saturation of aromatic ring at the relatively low temperature (180–210 °C) and moderate hydrogen pressure (0.5–3.0 MPa). Ni catalysts supported on silica materials exhibited a better deoxygenation activity with a HDO% of 70% for Ni/SBA-15 and 95% for Ni/SiO_2. Combination of acidic sites of the supports and good dispersion of the metal leads to a very good HDO yield over Ni/SiO_2, especially at high temperature (>200 °C). At the deficient H_2 pressure, even at the atmospheric pressure, the removal of —OCH_3 of anisole to form benzene by direct demethoxylation can also be achieved.

Acknowledgments

We gratefully acknowledge the financial support provided by the National Natural Science Foundation of China (21073023 and 21373038) and the Fundamental Research Funds for the Central Universities (DUT12YQ03).

References

[1] C. Zhao, Y. Kou, A.A. Lemonidou, X. Li, J.A. Lercher, Angew. Chem. 121 (2009) 4047–4050.
[2] Z. Xiao, S. Jin, M. Pang, C. Liang, Green Chem. 15 (2013) 891–895.
[3] W. Xu, S.J. Miller, P.K. Agrawal, C.W. Jones, ChemSusChem 5 (2012) 667–675.
[4] F.G. Calvo-Flores, J.A. Dobado, ChemSusChem 3 (2010) 1227–1235.
[5] K.L. Deutsch, B.H. Shanks, Appl. Catal. A: Gen. 447/448 (2012) 144–150.
[6] J. Zakzeski, P.C.A. Bruijnincx, A.L. Jongerius, B.M. Weckhuysen, Chem. Rev. 110 (2010) 3552–3599.
[7] H. Li, X.S. Chai, M. Liu, Y.H. Deng, J. Agric. Food Chem. 60 (2012) 5307–5310.
[8] V.N. Bui, G. Toussaint, D. Laurenti, C. Mirodatos, C. Geantet, Catal. Today 143 (2009) 172–178.
[9] E. Laurent, B. Delmon, Appl. Catal. A: Gen. 109 (1994) 77–96.
[10] O.I. Senol, T.R. Viljava, A.O.I. Krause, Catal. Today 100 (2005) 331–335.
[11] H. Ohta, H. Kobayashi, K. Hara, A. Fukuoka, Chem. Commun. 47 (2011) 12209–12211.
[12] X.L. Zhu, L.L. Lobban, R.G. Mallinson, D.E. Resasco, J. Catal. 281 (2011) 21–29.
[13] C.R. Lee, J.S. Yoon, Y.W. Suh, J.W. Choi, J.M. Ha, D.J. Suh, Y.K. Park, Catal. Commun. 17 (2012) 54–58.

Please cite this article in press as: S. Jin, et al., Catalytic hydrodeoxygenation of anisole as lignin model compound over supported nickel catalysts, Catal. Today (2014), http://dx.doi.org/10.1016/j.cattod.2014.02.014

[14] N. Yan, Y. Yuan, R. Dykeman, Y. Kou, P.J. Dyson, Angew. Chem. Int. Ed. 49 (2010) 5549–5553.
[15] K. Li, R. Wang, J. Chen, Energy & Fuels 25 (2011) 854–863.
[16] H.Y. Zhao, D. Li, P. Bui, S.T. Oyama, Appl. Catal. A: Gen. 391 (2011) 305–310.
[17] Y. Yang, J. Chen, H. Shi, Energy & Fuels 27 (2013) 3400–3409.
[18] Y. Yang, C. Ochoa-Hernández, V.A. de la Pen˜a O'Shea, J.M. Coronado, D.P. Serrano, ACS Catal. 2 (2012) 592–598.
[19] X.Y. Wang, R. Rinaldi, Energy Environ. Sci. 5 (2012) 8244–8260.
[20] P.T.M. Do, A.J. Foster, J. Chen, R.F. Lobo, Green Chem. 14 (2012) 1388–1397.
[21] I.T. Ghampson, C. Sepúlveda, R. Garcia, J.L. García Fierro, N. Escalona, W.J. Desisto, Appl. Catal. A: Gen. 435/436 (2012) 51–60.
[22] R.N. Olcese, M. Bettahar, D. Petitjean, B. Malaman, F. Giovanella, A. Dufour, Appl. Catal. B: Environ. 115/116 (2012) 63–73.
[23] P. Wu, T. Tatsumi, Chem. Mater. 14 (2002) 1657–1664.
[24] O. González, H. Pérez, P. Navarro, L.C. Almeida, J.G. Pacheco, M. Montes, Catal. Today 148 (2009) 140–147.
[25] A.L. Alberton, M.M.V.M. Souza, M. Schmal, Catal. Today 123 (2007) 257–264.
[26] A.R. Naghash, T.H. Etsell, S. Xu, Chem. Mater. 18 (2006) 2480–2488.
[27] Y. Cesteros, P. Salagre, F. Medina, J.E. Sueiras, Chem. Mater. 12 (2000) 331–335.
[28] E. Heracleous, A.F. Lee, K. Wilson, A.A. Lemonidou, J. Catal. 231 (2005) 159–171.
[29] Y. Qian, S. Liang, T. Wang, Z. Wang, W. Xie, X. Xu, Catal. Commun. 12 (2011) 851–853.
[30] Y.X. Yang, C. Ochoa-Hernández, V.A. de la Peña O'Shea, P. Pizarro, J.M. Coronado, D.P. Serrano, Appl. Catal. B: Environ. 145 (2013) 91–100.
[31] M.V. Bykova, D.Yu. Ermakov, V.V. Kaichev, O.A. Bulavchenko, A.A. Saraev, M.Yu. Lebedev, V.A. Yakovlev, Appl. Catal. B: Environ. 113/114 (2012) 296–307.
[32] C.V. Loricera, B. Pawelec, A. Infantes-Molina, M.C. Álvarez-Galván, R. Huirache-Acuña, R. Nava, J.L.G. Fierro, Catal. Today 172 (2011) 103–110.

Please cite this article in press as: S. Jin, et al., Catalytic hydrodeoxygenation of anisole as lignin model compound over supported nickel catalysts, Catal. Today (2014), http://dx.doi.org/10.1016/j.cattod.2014.02.014